Supporting Information for

Chirality Functionalization Coordinates with External Magnetic Field for Enhancing Oxygen Evolution Reaction of Water Electrolysis

Baowen Zhou [a, *], Ying Li [b], Lin Yao [b, *], Lufei Huang [b], Rui Tian [b], Liang Qiu [a], Ewa Mijowska [c], Xuecheng Chen [c], Wei Li [d]

[a] Key Laboratory for Power Machinery and Engineering of Ministry of Education, Research Center for Renewable Synthetic Fuel, School of Mechanical Engineering, Shanghai Jiao Tong University, 800 Dongchuan Road, Shanghai 200240, China.

[b] China-UK Low Carbon College, Shanghai Jiao Tong University, Shanghai 201306, China.

[c] Department of Nanomaterials Physicochemistry, Faculty of Chemical Technology and Engineering, West Pomeranian University of Technology, Szczecin, Piastow Ave. 45, 70-311 Szczecin, Poland.

[d] Institute for Materials and Processes, School of Engineering, The University of Edinburgh, Edinburgh, Scotland EH9 3FB, United Kingdom.

Methods

Synthesis of $CoFeO_x$

Firstly, $CoFeO_x$ was synthesized according to the traditional solid-state chemical method, and then different chiral ligands were bound to $CoFeO_x$ using an ultrasonic method reported in the literature to obtain chiral $CoFeO_x$.

(1) Synthesis of $CoFeO_x$

Firstly, a mixture of 9 mmol of $Fe(NO_3)_3 \cdot 9H_2O$ and $Co(NO_3)_2 \cdot 6H_2O$ was weighed in a certain proportion and added to 15 mL of deionized water to fully dissolve it. The mixture was then placed in a magnetic heating stirrer for stirring to evaporate the solvent, with the heating temperature set to 80°C. After obtaining a viscous slurry, it was placed in a muffle furnace and calcined at 250°C for 2 hours to completely decompose the nitrites. The obtained black oxide powder was then thoroughly ground and calcined again at 400°C for 8 hours. Subsequently, $CoFeO_x$ was obtained.

(2) Assembly of chiral $CoFeO_x$

Chiral molecules were linked to $CoFeO_X$ using an ultrasonic method. The same molar amounts of $CoFeO_x$ and different chiral ligands (D-penicillamine, D-cysteine, D-phenylethanolamine, abbreviated as D-pen, D-cys, D-phe, respectively) were weighed and added to 5 mL of ultrapure water, mixed uniformly. Ultrasonic waves were applied at a power of 100 W for 60 minutes. The obtained products were named $CoFeO_x$@D-phe, $CoFeO_x$@D-pen, and $CoFeO_x$@D-cys, respectively.

Characterization

The morphology underwent evaluation using JEOL-2100F for transmission electron microscopy (TEM) and SU8100 (Hitachi, Japan) for scanning electron microscopy (SEM). Determination of the sample's composition was achieved through energy-dispersive spectroscopy (EDS) experiments conducted within the TEM. Further analysis, including high-resolution HAADF-STEM and EDS-mapping, was performed using the STEM mode of a JEOL JEM-ARM 300F with double aberration correctors and two EDS detectors, each of which had an active area of 100 mm^2. X-ray diffraction (XRD) patterns of the synthesized materials were obtained utilizing a Bruker D8

Advance. X-ray diffractometer equipped with a Cu target and a ceramic X-ray tube, operating at an accelerating voltage of 60 kV and an emission current of 80 mA. X-ray photoelectron spectroscopy (XPS) analysis was carried out on a ESCALAB 250xi instrument equipped with non-monochromatic Al Kα (Photon energy of 1486.6 eV). The MPMS-VSM from Quantum Design was used to test the hysteresis loop of $CoFeO_x$ at a temperature of 300K and a magnetic field strength ranging from -2 to 2 Tesla. Circular dichroism (CD) spectra were obtained using a JASCO J-815 spectrometer at room temperature. Three scans were collected and averaged for each measurement with a bandwidth of 1.00 nm and at a rate of 100 nm/min. UV-vis diffuse reflectance spectra, measured on a Persee T-700 spectrometer, examined the light adsorption properties of the catalysts. The magnetic field for the electrochemical tests is provided by EM4WP electromagnet from Dongfang Chenjing.

Electrochemical testing

Take a certain amount of different mixtures, place them in a 2 mL mixture of isopropanol and water with a volume ratio of 1:1, add 50 uL of nafion solution, mix thoroughly under ultrasound, and evenly apply it to a 1 cm × 1 cm treated foam nickel. The foam nickel was dried at room temperature overnight for testing. The experiment uses a Gamry 1010E electrochemical workstation, with 1 M KOH solution as the electrolyte, Hg/HgO electrode as the reference electrode, carbon rod as the counter electrode, and catalyst-loaded foam nickel as the working electrode. When conducting formal electrochemical testing, first perform cyclic voltammetry (CV) scanning until the curve stabilizes. The potential range is set to 0.35 V to 1 V vs. Hg/HgO. The scanning rate is 50 mV/s. In the CI compensation mode, a linear sweep voltammetry LSV scan was performed at a scan rate of 5 mV/s. To unify the potential standard, the potential in all test results is converted to the reversible hydrogen electrode (RHE) potential using the Nernst equation. The Tafel slope is calculated using the Tafel equation.

DFT calculation

Density functional theory (DFT) calculations were carried out using the Vienna Ab

initio Simulation Package (VASP)[1]. The Perdew–Burke–Ernzerhof (PBE) functional was employed to describe the exchange-correlation energy, while the projector augmented-wave (PAW) method was adopted to treat the ion-electron interactions[2]. For all geometry optimizations, the cut-off energy for plane-wave expansion was set to 500 eV. The convergence criterion for atomic forces was set to below 0.02 eV/Å, with an iterative energy convergence threshold of 10^{-5} eV. Based on the characterization results, the CoFeOx model was constructed by integrating the (001) facet of Fe_2O_3 and Co_3O_4. Brillouin zone sampling was performed using a 2×2×1 Gamma-centered grid for the (001) surface of $CoFeO_x$. A vacuum layer of at least 20 Å was introduced along the z-direction of the slab models to avoid vertical interactions between adjacent slabs. The spin alignment during structural relaxation was controlled by applying a magnetic field to the model via the "MAGMOM" parameter. Post-processing of the calculation results was conducted using the VASPKIT package.

The four electron reaction steps for the OER process are as follows[3]:

H_2O (l) + M_1* → M_1OH* + e^- + H^+ (1)

M_1OH* → M_1O* + e^- + H^+ (2)

H_2O (l) + M_1O* → M_1OOH* + e^- + H^+ (3)

M_1OOH* → O_2 (g) + e^- + H^+ + M_1* (4)

The calculation of the Gibbs free energy of adsorption (ΔG) was conducted using the following formula:

$$\Delta G = E_{ad} + \Delta ZPE - T\Delta S \quad (5)$$

where Ead is the adsorption energy defined by:

$$E_{ad} = E_{surface+adsorbate} - E_{surface} - E_{adsorbate} \quad (6)$$

ΔZPE and ΔS are the changes in zero-point energy and entropy during adsorption.[4, 5]

The overpotential (η^{OER}) employed to further validate the catalytic activity of OER can be calculated by using the subsequent equations:

η^{OER} = max {ΔG1, ΔG2, ΔG3, ΔG4}/e – 1.23 (7)

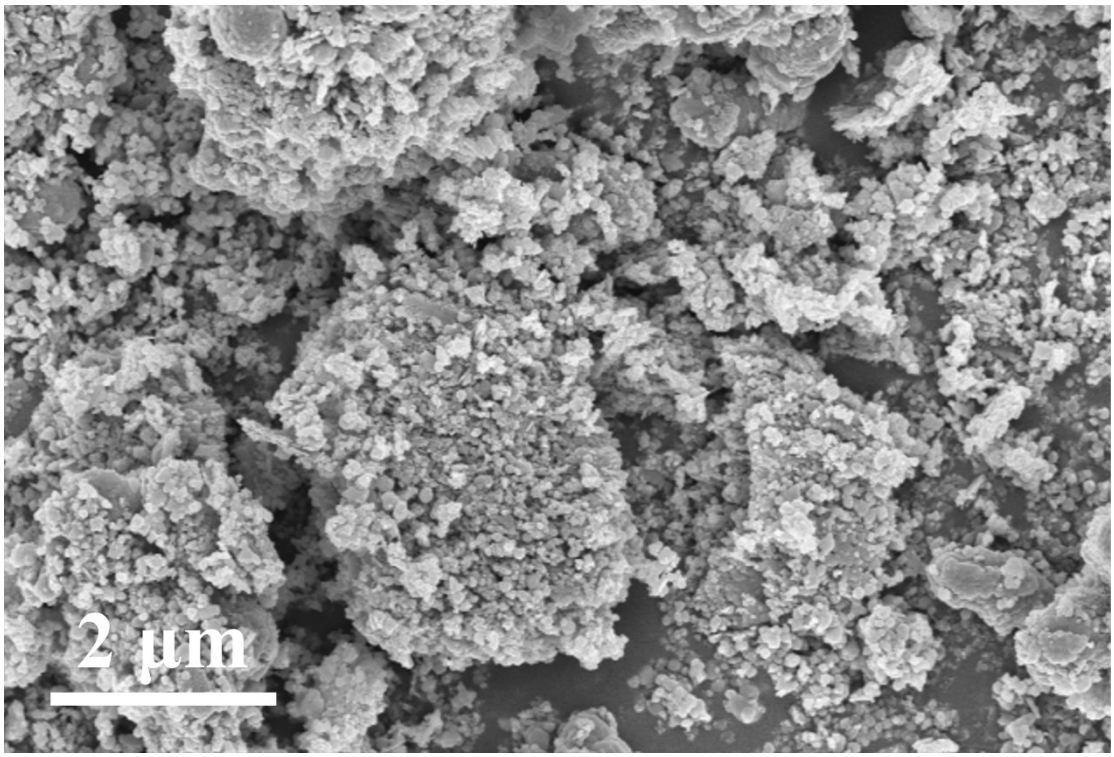

Figure S1 The SEM image of the powdered $CoFeO_x$ appears granular, with an approximate diameter of 100 nm.

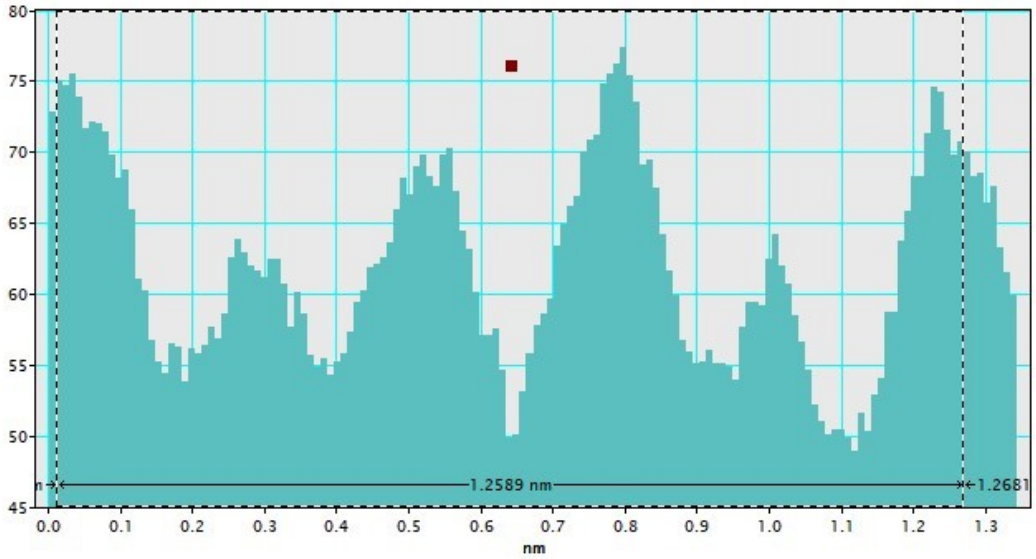

Figure S2 The total length of the 5 lattice lines is 1.2589 nm, and the lattice spacing in Fig. 1b is 0.2518 nm. This value corresponding to the (110) crystal plane of Fe_2O_3.

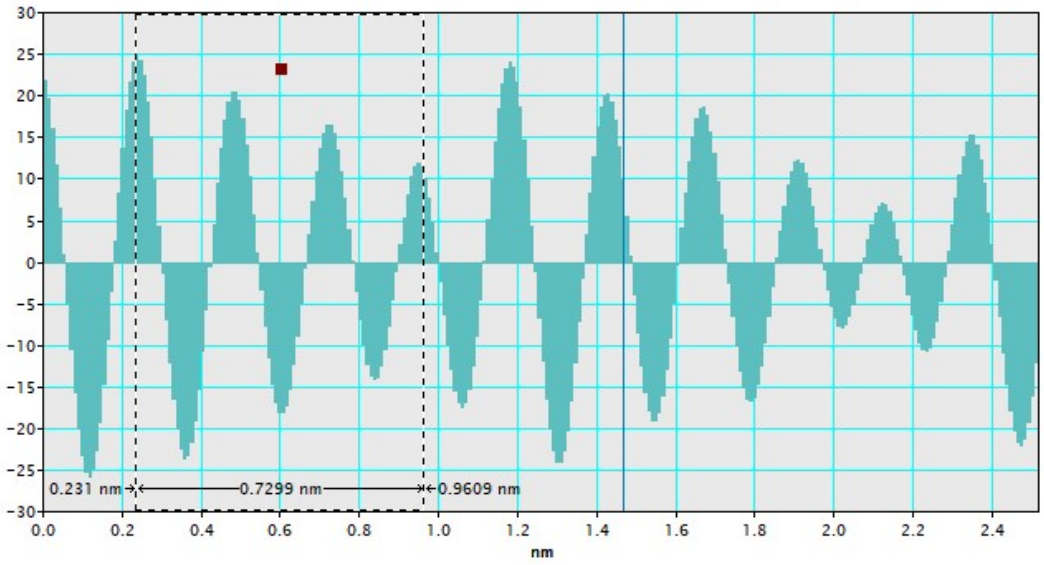

Figure S3 The total length of the 3 lattice lines is 0.7299 nm, and the lattice spacing in Fig. 1b is 0.2433 nm. This value corresponding to the (311) crystal plane of Co_3O_4.

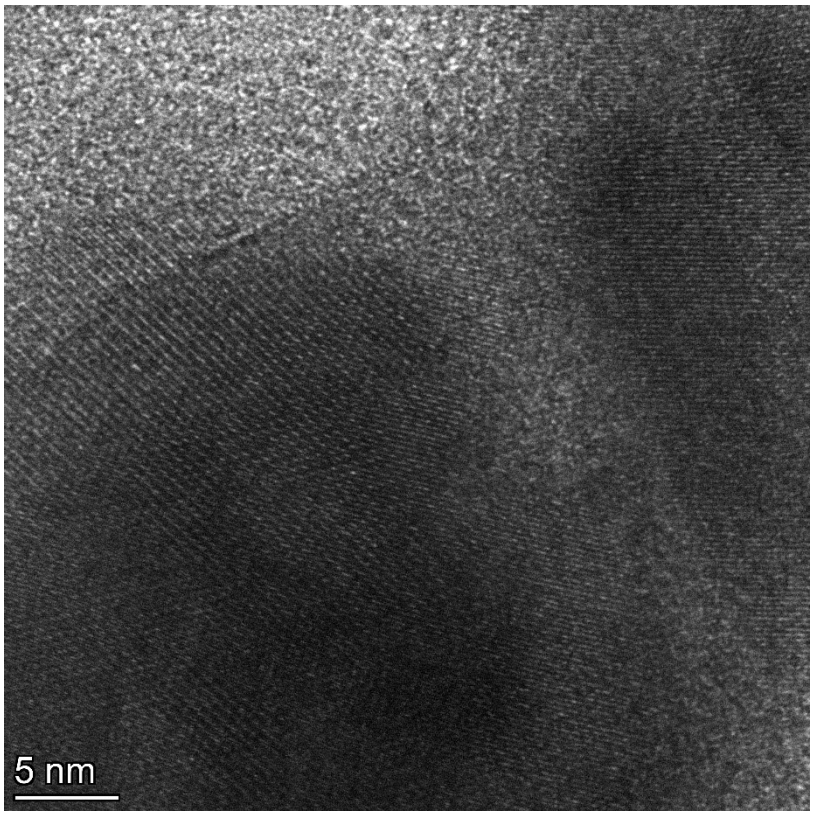

Figure S4 The HRTEM image of the powdered $CoFeO_x$, the lattice spacing is 0.2518 nm. This value corresponding to the (110) crystal plane of Fe_2O_3.

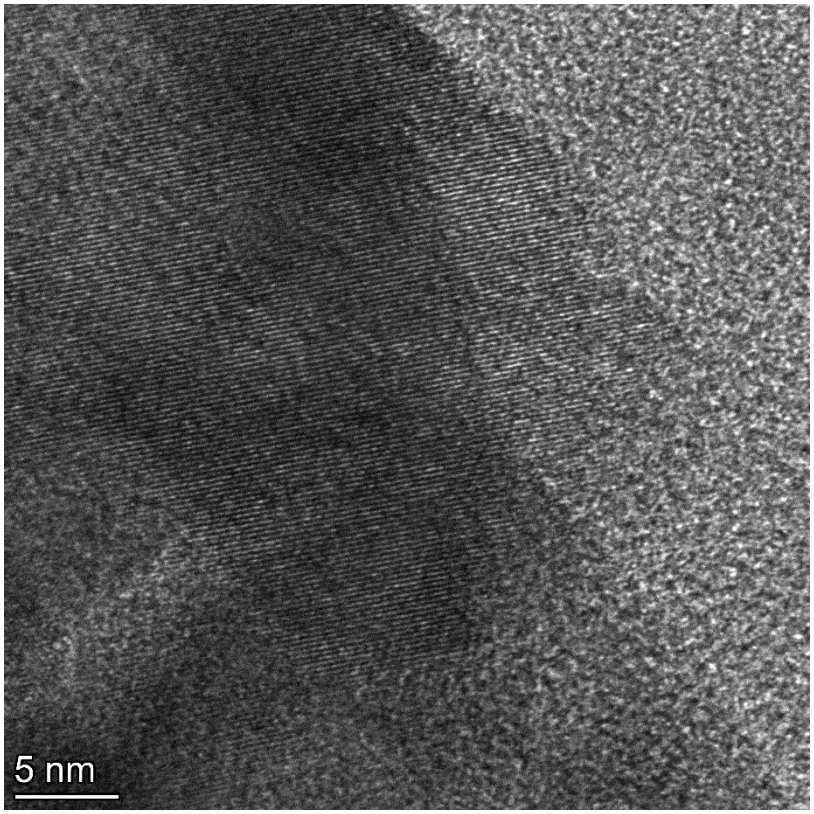

Figure S5 The HRTEM image of the powdered $CoFeO_x$, the lattice spacing is 0.243 nm. This value corresponding to the (311) crystal plane of Co_3O_4.

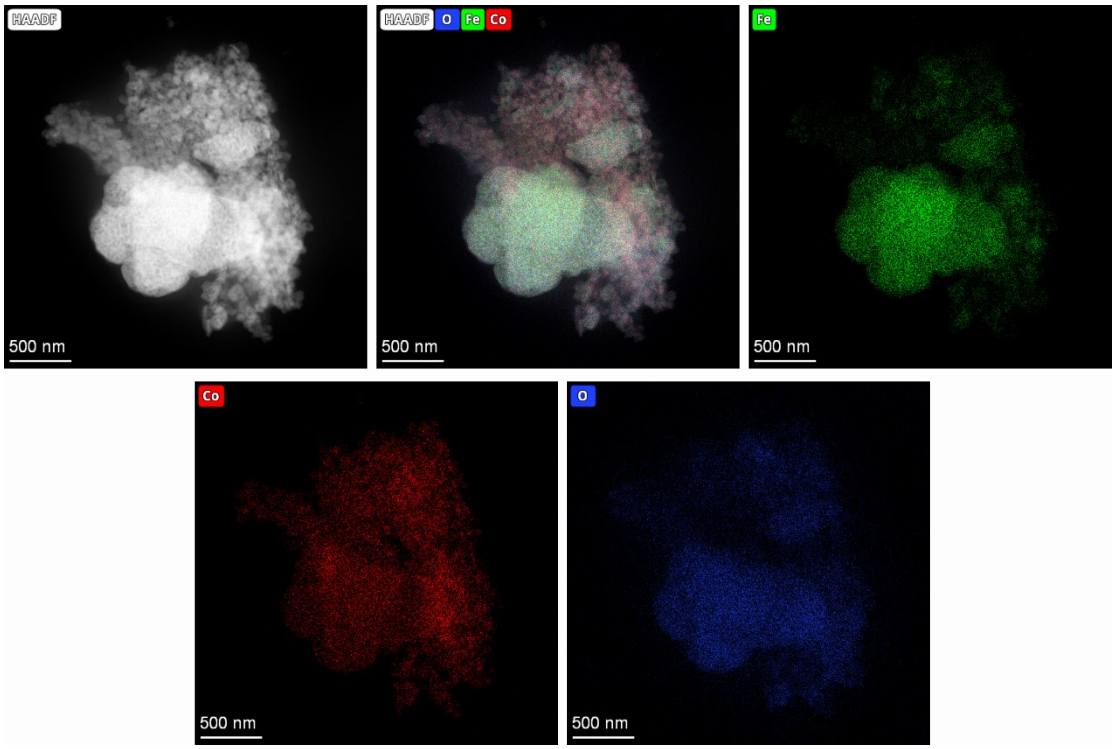

Figure S6 The EDS patterns of $CoFeO_x$ NPs.

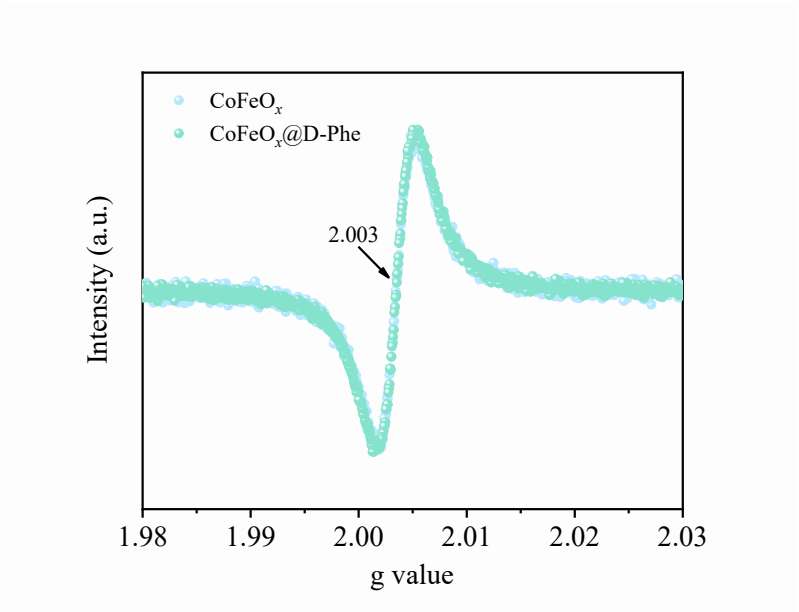

Figure S7 The EPR spectra of $CoFeO_x$ and $CoFeO_x$@D-Phe.

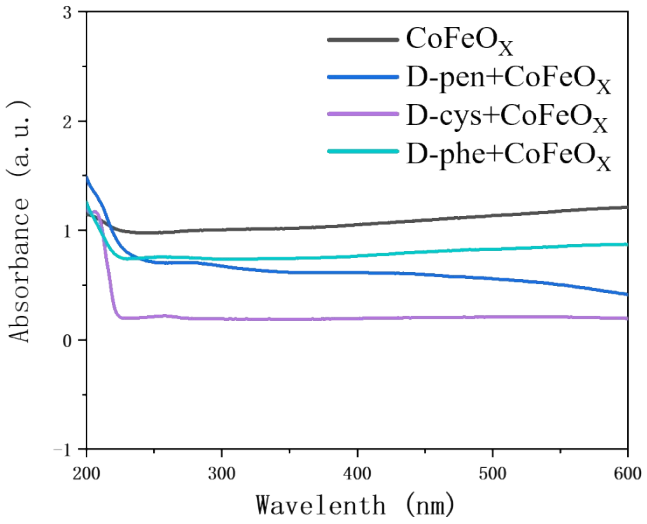

Figure S8 UV-Vis spectra of $CoFeO_x$ NPs, $CoFeO_x$@D-Pen, $CoFeO_x$@D-Phe, and $CoFeO_x$@D-Cys.

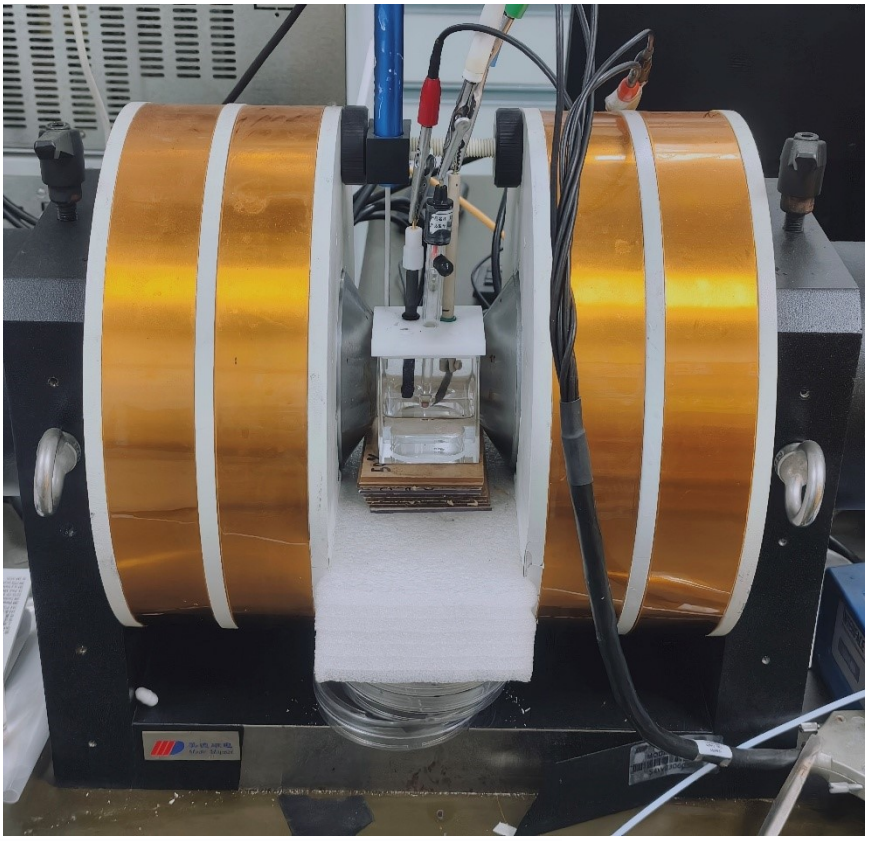

Figure S9 Photo of catalyst test under magnetic field.

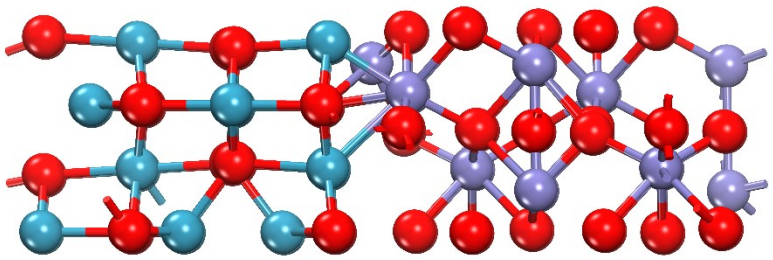

Figure S10 The model structures of $CoFeO_x$.

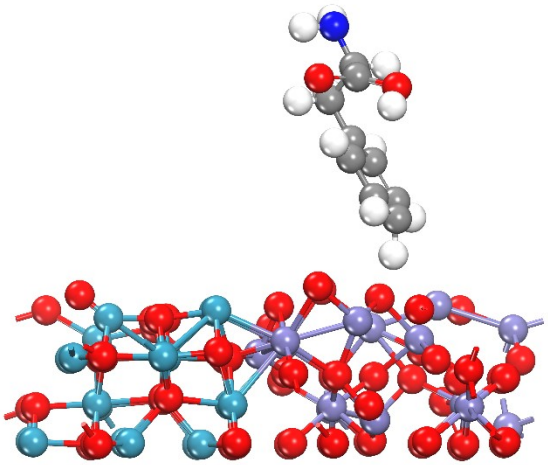

Figure S11 The model structures of $CoFeO_x$@D-Phe.

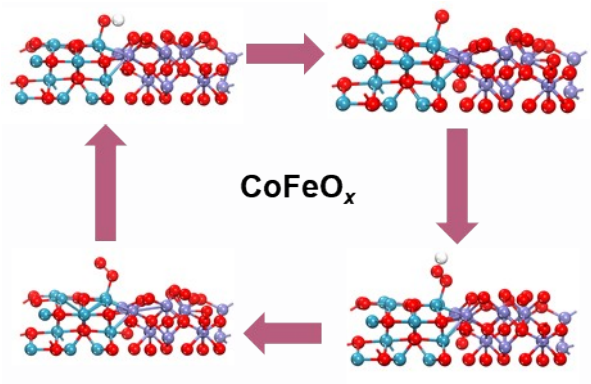

Figure S12 The schematic OER pathways of $CoFeO_x$.

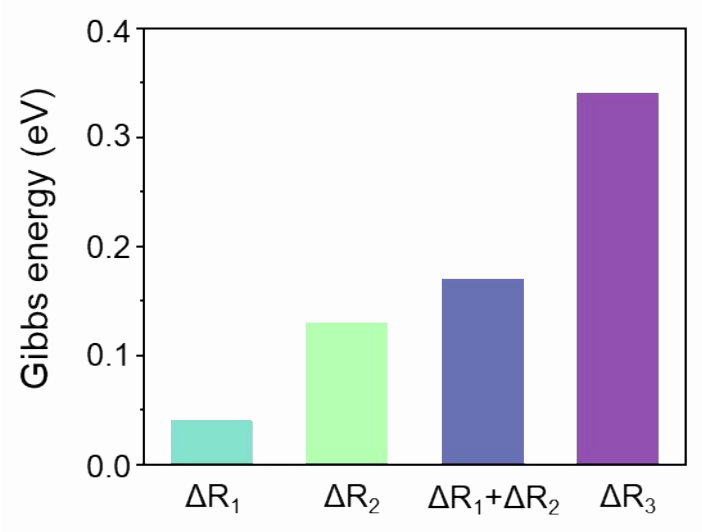

Figure S13 Histogram showing the RDS energy barrier reduction amplitudes (eV) of $CoFeO_x$-based systems vs. pure $CoFeO_x$: ΔR1 ($CoFeO_x$+M, 0.04 eV), ΔR_2 ($CoFeO_x$@D-Phe, 0.13 eV), $\Delta R_1+\Delta R_2$ (additive effect, 0.17 eV), and ΔR_3 ($CoFeO_x$@D-Phe+M, 0.34 eV). $\Delta R_3 > \Delta R_1+\Delta R_2$, confirming the synergistic effect of chiral functionalization and external magnetic field.

Table S1. Chiral Molecules Used

Chiral molecules	Molecular formula	Structural scheme
D-Penicillamine	$C_5H_{11}NO_2S$	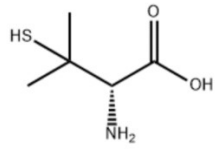
D-Cysteine	$C_3H_7NO_2S$	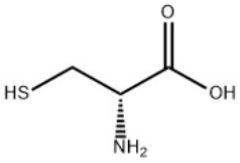
D-Phenylpropanol	$C_9H_{13}NO$	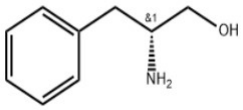

Table S2. The chirality-induced increase in current density (j_1) of $CoFeO_x$@D-Pen, $CoFeO_x$@D-Cys, and $CoFeO_x$@D-Phe at 1.65 V vs RHE.

	D-Pen	**D-Cys**	**D-Phe**
j_1	10.3	14.2	26.3

Table S3. The magnetic fields of 0.2T, 0.4T, 0.6T, and 0.8T resulted in current density increases (j_2) at 1.65 V vs RHE.

	0.2 T	**0.4 T**	**0.6 T**	**0.8 T**
j_2	8.2	14.1	20.4	24.0

Table S4. The calculated sum ($j_1 + j_2$) of current density increasing due to the chirality (j_1) and magnetic field (j_2) of $CoFeO_x$@D-Pen, $CoFeO_x$@D-Cys, and $CoFeO_x$@D-Phe at 1.65 V vs RHE.

	D-Pen	**D-Cys**	**D-Phe**
0.2 T	18.5	22.4	34.5
0.4 T	24.4	28.3	40.4
0.6 T	30.7	34.6	46.7
0.8 T	34.3	38.2	50.4

Table S5. At 1.65 V vs RHE, the current density of the combined enhancement effect of the chiral effect and the magnetic field effect (j_3).

	D-Pen	D-Cys	D-Phe
0.2 T	27.0	25.4	52.6
0.4 T	38.4	33.9	63.1
0.6 T	44.3	41.3	66.0
0.8 T	62.6	59.2	76.8

Reference

1. W. Kohn and L. J. Sham, Physical Review, 1965, 140, A1133-A1138.
2. G. Kresse and D. Joubert, Physical Review B, 1999, 59, 1758-1775.
3. Y. Li, S. H. Talib, D. Liu, K. Zong, A. Saad, Z. Song, J. Zhao, W. Liu, F. Liu, Q. Ji, P. Tsiakaras and X. Cai, Applied Catalysis B: Environmental, 2023, 320, 122023.
4. J. K. Nørskov, J. Rossmeisl, A. Logadottir, L. Lindqvist, J. R. Kitchin, T. Bligaard and H. Jónsson, The Journal of Physical Chemistry B, 2004, 108, 17886-17892.
5. V. Wang, N. Xu, J.-C. Liu, G. Tang and W.-T. Geng, Computer Physics Communications, 2021, 267, 108033.